Materialographic investigations of plate slags from the Late Bronze Age copper production site of Prigglitz-Gasteil (Lower Austria)

Roland Haubner [a,*], Susanne Strobl [a], Peter Trebsche [b]

[a] *TU Wien, Institute of Chemical Technologies and Analytics, A-1060 Vienna, Austria*
[b] *Leopold-Franzens-Universität Innsbruck, Institute of Archaeologies, Langer Weg 11, A-6020 Innsbruck, Austria*

ARTICLE INFO

ABSTRACT

This paper presents the microstructures and chemical analyses of 10 plate slags from the Late Bronze Age copper production site of Prigglitz-Gasteil in Lower Austria. The analytical results of overview measurements (XRF) and local measurements on metallographic samples (SEM-EDX) are compared. The samples belong to the category of thin plate slags (PS-C, thickness < 0.5 cm) and the newly defined category of very thin plate slags (PS-D, thickness < 0.2 cm). From their chemical and phase composition, three groups could be distinguished. These different groups did not indicate separate stages during the working process but rather haphazard variations. The amount of residual Cu observed in all the plate slags was small (average Cu content 0.59 wt%), indicating an efficient process of copper smelting, comparable with other prehistoric copper production sites in the Eastern Alps. Remarkably, some of the investigated plate slags contained Sn as a trace element which most likely came into the slag through contamination from the nearby bronze processing. In line with previous archaeometallurgical investigations, the analysis of plate slags confirms that primary and secondary metallurgy were carried out in immediate vicinity at the Prigglitz-Gasteil site.

1. Introduction

During the Bronze Age, copper production flourished in the Eastern Alps and left many impressive extraction sites along with numerous smelting sites for the reduction of copper ores to the valuable copper. Smelting techniques made an important step forward in the Bronze Age when a coincident technology for smelting sulphidic ores (mainly chalcopyrite) in shaft-furnaces was developed, probably in the Mitterberg region in the Salzach Valley (in today's State of Salzburg in Austria). This techno-complex subsequently spread to many other mining regions in the Eastern Alps (STÖLLNER, 2015; Pernicka, et al., 2016). Apart from the smelting furnaces and associated pottery products, slags are the only remains of prehistoric copper smelting in most archaeological contexts (HAUPTMANN, 2014). In the last two decades, the archaeological classification of slag from copper production (i.e., based on macroscopic, morphological evaluation, without instruments) has been refined by several authors (METTEN, 2003; Hanning, et al., 2015; REITMAIER-NAEF, 2019). Broadly speaking, copper production slags can be divided into slag cakes, massive slag, plate slag and slag sand, i.e., crushed slag (REITMAIER-NAEF, 2019).

In parallel with their archaeological classification, archaeological slags have also been investigated using a number of archaeometallurgical methods (e.g. Piel, et al., 1992; METTEN, 2003; Presslinger and Prochaska, 2002; Presslinger and Eibner, 2013/2014; Kraus, et al., 2015; Krismer, et al., 2015; Larreina-Garcia, et al., 2015; HERDITS, 2017). The main scientific debate centres on the question of whether the different slag types resulted from different copper smelting processes, different stages of one specific copper smelting process, or different copper ores (Haubner et al. 2015; HAUBNER, 2021). According to a recent study of smelting sites in Grisons in Switzerland, the different slag types resulted from two different stages in the copper smelting process: first, amorphous slag cakes were formed during reduction in the shaft furnaces; secondly, massive slag and plate slag were removed during the smelting process in an open reactor (REITMAIER-NAEF, 2019).

In this paper, we present archaeometallurgical analyses of a series of 10 plate-slag fragments from the copper production site of Prigglitz-Gasteil in southeastern Lower Austria (Fig. 1). This site is located on the eastern slope of the Gahns mountain in the Schneeberg-Rax region.

Various copper smelting sites were investigated in this region as early as the 1950 s, including Prigglitz-Gasteil. During these investigations, copper smelting in Prigglitz-Gasteil could be proven and

---

* Corresponding author.
E-mail address: roland.haubner@tuwien.ac.at (R. Haubner).

typical smelting slags were also found. At that time, however, no copper mine could be located (Hampl and Mayrhofer, 1958).

Geophysical prospections and core drillings conducted in 2017 and 2018 found evidence of an opencast copper-ore mine which was operated in several phases from ca. 1050 to 780 BCE, i.e., during the younger Urnfield Culture of the Late Bronze Age (Trebsche and Weixelberger, 2022; Trebsche et al., 2022). Immediately next to the opencast mine, a mining camp or settlement had developed. On top of the mining heaps, horizontal terraces had been created for building dwellings and

workshops. Two of the terrain terraces were partially excavated from 2010 to 2014, revealing abundant evidence of the life circumstances of Bronze Age miners and the organisation of copper production. Interdisciplinary analyses of the food remains (Trebsche and Pucher, 2013; Heiss, et al., 2021) and the metallurgical finds were conducted in the context of the Austrian Science Fund project "Life and Work at the Bronze Age Mine of Prigglitz" (project number P30289-G25). The project also included analyses of copper ores, casting cakes, casting debris, bronze finished products and slags for the purpose of
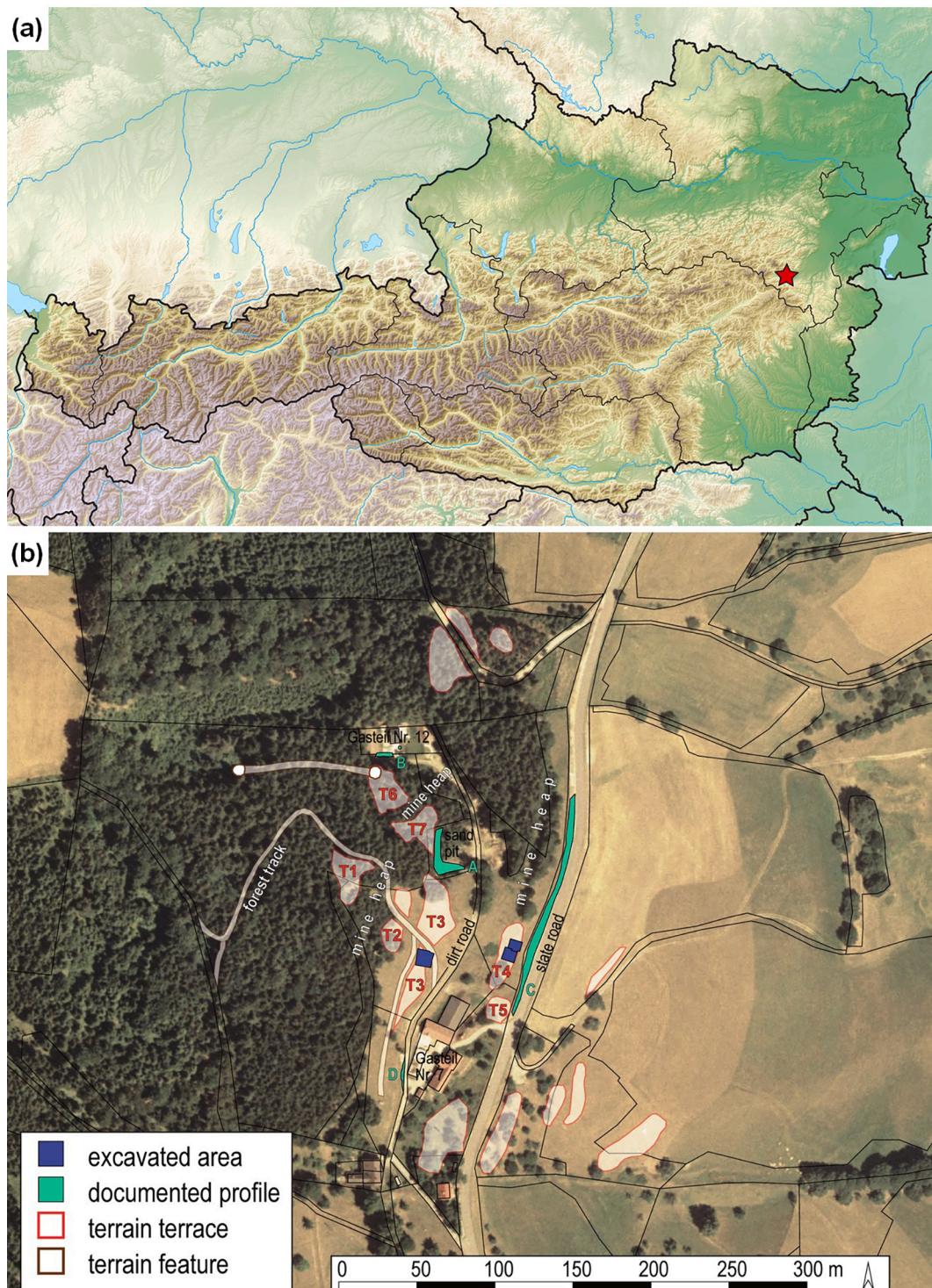

Fig. 1. Prigglitz-Gasteil. (a) Location in Austria, (b) plan of the site showing terrain terraces (T), dumps, excavation areas, and core drilling sites (KB). – (map of Austria: © BEV, 2021 with kind permission; orthophoto: © Land Niederösterreich with kind permission; additions by Peter Trebsche).

determining the *chaîne opératoire* of copper production and bronze working (Haubner, et al., 2019). Analyses of the copper and bronze artefacts revealed that the copper produced at Prigglitz-Gasteil was distributed and worked throughout the region surrounding the copper ore mine, and possibly beyond, while at the same time copper alloy artefacts of different origin were recycled in the casting workshops located at Prigglitz-Gasteil (Mödlinger and Trebsche, 2021; Mödlinger, et al., 2021).

Among the metallurgical finds excavated at Prigglitz-Gasteil from 2010 to 2014, slags were the most numerous find category (444 fragments with a total weight of 3489 g), followed by ca. 200 casting drops and 47 other copper or copper alloy artefacts (Haubner, et al., 2019; Mödlinger, et al., 2021) and other casting debris. Almost all the slags (96 %) from the excavations of 2010 to 2014 belonged to the type of plate slags. It should be mentioned, however, that the excavated ensemble

was not necessarily representative of the whole copper production site, as one complete slag cake with a diameter of ca. 25 cm and a thickness of 2 cm was found during road construction works in the year 2000 (Lang, 2000, 596).

Most of the plate slags belonged to the types PS-B (0.5–0.95 cm thickness) and PS-C (0.2–0.45 cm thickness) defined by Reitmaier-Naef (2019). However, a significant proportion (27 %) were thinner than 0.2 cm and should therefore be grouped into a separate type PS-D (<0.2 cm thickness) which apparently did not occur in Reitmaier-Naef's study area in Grisons.

For our analyses, 10 fragments of plate slags were randomly selected from two different terrain terraces. Five plate slags (sample numbers Pr 156, 199–1, 199–2, 209 and 215) were found in stratigraphic unit 43 in excavation area 1 on terrain terrace T4. They belonged to the building phase T4-09, which dated, according to a high-resolution series of
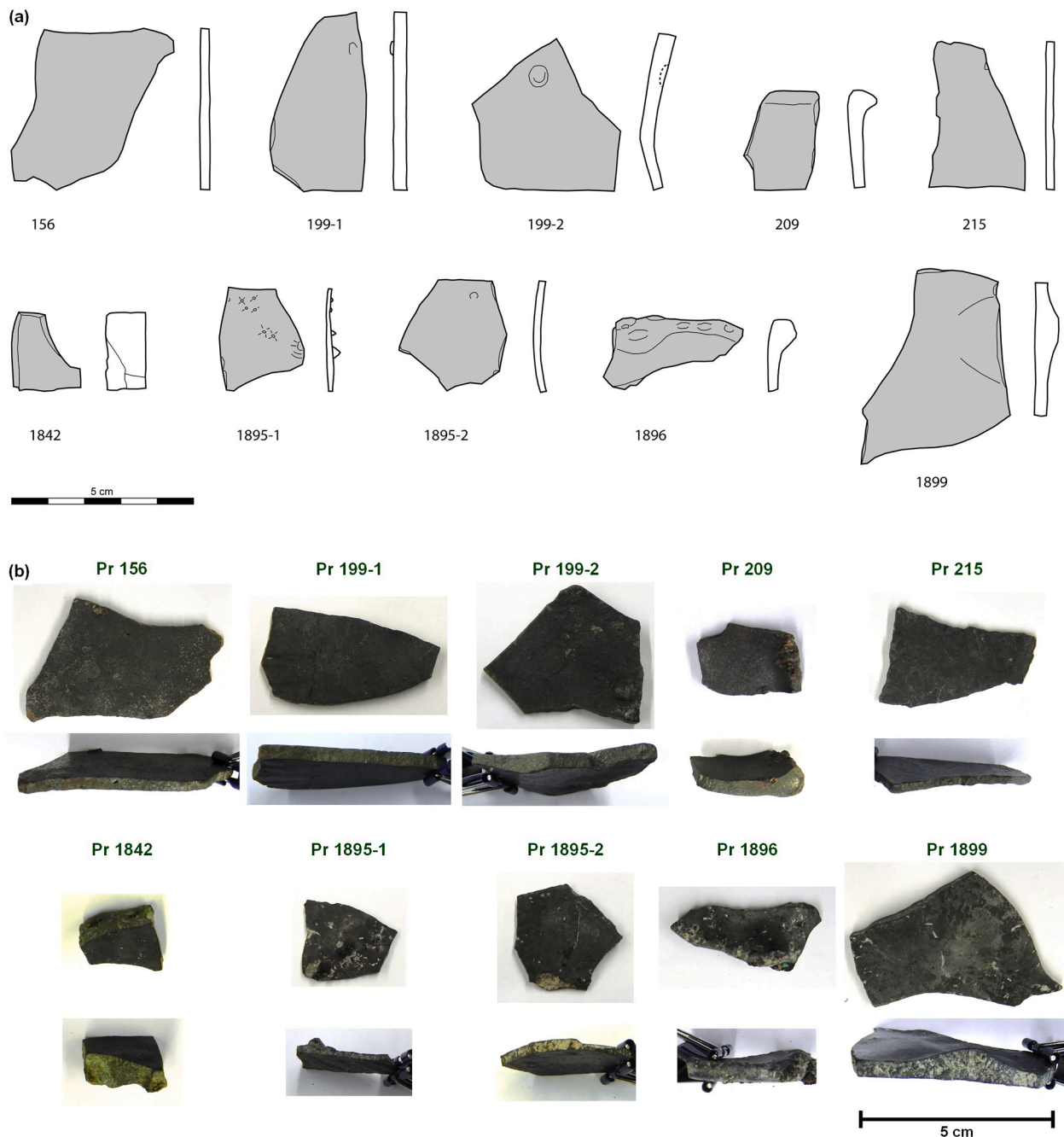

Fig. 2. Drawings (a) and photographs (b) of the investigated slag fragments from Prigglitz-Gasteil. Top and side views.

radiocarbon analyses, from ca. 900 BCE and lasted for a very short period of ca. 5–10 years. The other five plate-slag samples belonged to stratigraphic unit 915 (Pr 1842) from building phase T3-08E and to stratigraphic unit 916 (Pr 1895–1, 1895–2, 1896, 1899) from the preceding phase, T3-08F. Phase T3-08F dated from the time period around 900–860 BCE, while phase T3-08E was slightly younger (860–850 BCE). The possibility cannot be excluded, however, that finds attributed to the latter phase, T3-08E, were, in fact, older finds from the second half of the 11th century or the first half of the 10th century BCE that had been redeposited on terrace 3.

The aim of the archaeometallurgical investigation of the plate slags was to resolve the following research questions: During what stage of copper production were the plate slags formed? What kind of copper ores were used for metal production at Prigglitz-Gasteil? How and at what temperature did the slags solidify? How efficient was the copper production process? Were there technological differences between the slags from the two different terrain terraces? Was there any variability in plate slag composition at the intra-site level and at the inter-site level (compared with other Bronze Age copper smelting sites in the Eastern Alps)?

2. Sample preparation and examination methods

From the Prigglitz-Gasteil excavation ten slags were available for material investigations (Fig. 2, Table 1). The surfaces of the slags were first documented with a 3D digital microscope (3D DM) (KEYENCE VHX-5000). Some were then also examined in a scanning electron microscope (SEM) (company FEI) with a backscattered electron detector (SEM-BSE) and by energy-dispersive X-ray analysis (SEM-EDX) (company EDAX).

For the metallographic investigations, the slags were cut with a cutting machine using a diamond saw blade. After cold mounting with epoxy resin, the specimens were ground and polished step by step up to 1 μm diamond and examined in the polished state using a light optical microscope (LOM) (Olympus GX51 with an associated CCD camera), and SEMEDX. The SEM worked in low vacuum mode to avoid charging. 20 or 25 kV were selected as the acceleration voltage for the electrons. At EDX, the light elements are recorded less accurately than heavy elements. Furthermore, it should be considered that, depending on the sample material, a certain volume around the point of impact of the electrons is also measured (HODOROABA, V.-D., 2020). In order to reduce this inaccuracy, area measurements were carried out.

The elemental compositions of the slags were also determined by X-ray fluorescence analyses (XRF). A Panalytical Axios Advanced machine

was used, working with a wavelength dispersive X-ray spectrometer, a Rh tube, an excitation voltage of 50 kV, a tube current of 50 mA and in < 10 Pa vacuum. The metallographically prepared samples were measured and the irradiated area circle had a diameter of 10 mm. The Panalytical Omnian standards and Panalytical Omnian software were used. For measuring the element Sn the Kα line, a LiF 200 analyzer crystal and a scintillation counter were deployed.

To compare the chemical compositions of the slags, the FeO-SiO$_2$-CaO phase diagram was used. In previous work it had been shown that the Al$_2$O$_3$ and MgO contents should be included in the calculation of the CaO to give realistic values for melting temperatures in the phase diagram (Haubner, et al., 2019).

3. Results

Bronze Age copper slags can be classified according to different criteria, taking into account the particularities of the measurement methods used (Haubner, et al., 2017a). For example, XRF gives accurate results for the chemical composition of larger sample volumes, where the samples are homogeneous. In the case of inhomogeneous samples, fluctuating measurements are obtained, depending on the random arrangement in the area or volume being measured.

SEM-EDX allows very local measurements, but fluctuations in the results may also occur if there is local inhomogeneity. If the SEM-EDX measurements are combined with light optical micrographs, the slag properties can be estimated.

In the following chapters, the results of the slag analyses are considered from various points of view.

3.1. Evaluation of the XRF measurements

Table 2 summarises the XRF measurement results from the ten slags. The analysis results are shown in the FeO-SiO$_2$-CaO phase diagram (Fig. 3a). It should be noted that the contents of CaO, MgO and Al$_2$O$_3$ were added together (Haubner, *et al.*, 2017b) and that the positions of the points in the phase diagram give only a rough indication of the melting and solidification behaviour of the slags.

The slags could be roughly divided into three groups based on their compositions and their positions in the phase diagram:

Group 1: Composition around the ternary eutectic olivine-wollastonite-SiO$_2$ (1105 °C) (Pr 199–2, Pr 215, Pr 1895–1, Pr 1895–2).

Group 2: Composition at the olivine-wustite phase boundary (1100–1150 °C) (Pr 199–1, Pr 209, Pr 1896, Pr 1899).

Group 3: Composition in the phase area of wustite (1250–1300 °C)

Table 1
Description of the investigated plate slag fragments from Prigglitz-Gasteil.

Find no.	Length [cm]	Width [cm]	Thickness [cm]	Weight [g]	Colour	Remarks
156	5.66	3.33	0.22–0.27	10.67	steel-grey	one brownish grey inclusion
						(0.4 × 0.3 cm)
199–1	4.75	2.54	0.33–0.37	11.62	steel-grey	one side slightly corrugated, on the other side two small bulges
						(max. thickness 0.44 cm)
199–2	4.05	3.96	0.24–0.48	14.01	steel-grey	flexed, one small depression
209	2.63	1.90	0.33	5.55	one side steel-grey,	thickened rim, on the outside of the
					other side brownish grey	rim rubiginous
215	3.88	2.63	0.22–0.25	5.65	steel-grey	one side slightly corrugated
1842	1.97	1.71	1.03	7.70	steel-grey	one side corroded green
1895–1	2.68	2.27	0.13–0.18	2.83	brownish grey	spiky protuberances on one side
						(max. thickness 0.41 cm)
1895–2	3.17	2.84	0.19–0.25	5.33	greenish grey	slightly convex
1896	3.35	1.83	0.28	6.14	steel-grey	irregularly thickened rim
						(thickness 0.46 cm, max. 0.74 cm)
1899	5.27	4.06	0.30	16.33	steel-grey	one bulge (max. thickness 0.66 cm)

Table 2
Result of the XRF measurements in wt.% of the plate slag fragments from Prigglitz-Gasteil. (ldl = lower detection limit).

	Pr 156	Pr 199–1	Pr 199–2	Pr 209	Pr 215	Pr 1842	Pr 1895–1	Pr 1895–2	Pr 1896	Pr 1899
Fe_2O_3	61.03	59.59	48.11	50.05	45.49	66.95	46.68	44.36	53.25	54.48
SiO_2	19.48	26.89	33.61	27.07	37.51	15.07	37.50	39.57	26.67	27.35
Al_2O_3	1.53	1.63	5.15	2.67	3.48	2.11	3.13	3.36	1.82	2.06
CaO	10.82	3.84	3.66	11.20	5.07	8.74	5.27	5.01	9.28	8.88
MnO	1.36	1.58	1.31	1.76	0.98	0.45	0.94	0.86	1.60	1.48
MgO	0.58	1.03	1.72	1.38	0.99	0.51	0.58	0.58	0.60	0.85
Na_2O	0.45	0.21	0.49	0.17	0.37	0.22	0.23	0.65	0.23	0.22
K_2O	1.62	2.30	1.57	2.62	1.17	2.46	1.31	1.24	3.84	2.42
CuO	0.75	0.63	0.49	1.19	0.35	0.35	0.39	0.38	0.77	0.55
Co_3O_4	ldl	ldl	0.04	ldl.	0.05	0.11	0.05	0.04	ldl	ldl
P_2O_5	0.10	0.09	0.23	0.11	0.28	0.57	0.34	0.35	0.19	0.08
TiO_2	0.20	0.20	0.22	0.31	0.14	0.33	0.13	0.14	0.38	0.27
NiO	0.05	ldl	ldl	ldl	0.01	0.02	0.01	0.01	ldl	ldl
SO_3	1.93	1.93	2.81	1.46	2.99	1.20	2.75	2.90	1.34	1.35
V_2O_5	ldl	0.01	ldl	ldl	ldl	0.02	ldl	ldl	ldl	ldl
Cr_2O_3	0.02	0.02	0.01	0.01	0.01	0.03	0.01	0.01	0.01	ldl
ZnO	0.03	0.02	0.01	ldl	0.01	0.02	0.02	0.02	0.01	0.01
SrO	ldl	ldl	0.09	ldl	0.40	ldl	0.45	0.23	ldl	ldl
ZrO_2	ldl	ldl	ldl	ldl	0.01	ldl	0.01	ldl	ldl	ldl
PbO	ldl	0.02	ldl	ldl	ldl	0.80	ldl	ldl	0.02	ldl
Sb_2O_3	ldl	ldl	0.01	ldl	0.03	ldl	0.03	0.04	ldl	ldl
SnO	0.06	ldl	0.08	ldl	0.44	ldl	ldl	0.18	ldl	ldl
Rb_2O	ldl	ldl	0.06	ldl	0.22	ldl	0.20	0.09	ldl	ldl
As_2O_3	ldl	ldl	ldl	ldl	ldl	0.04	ldl	ldl	ldl	ldl
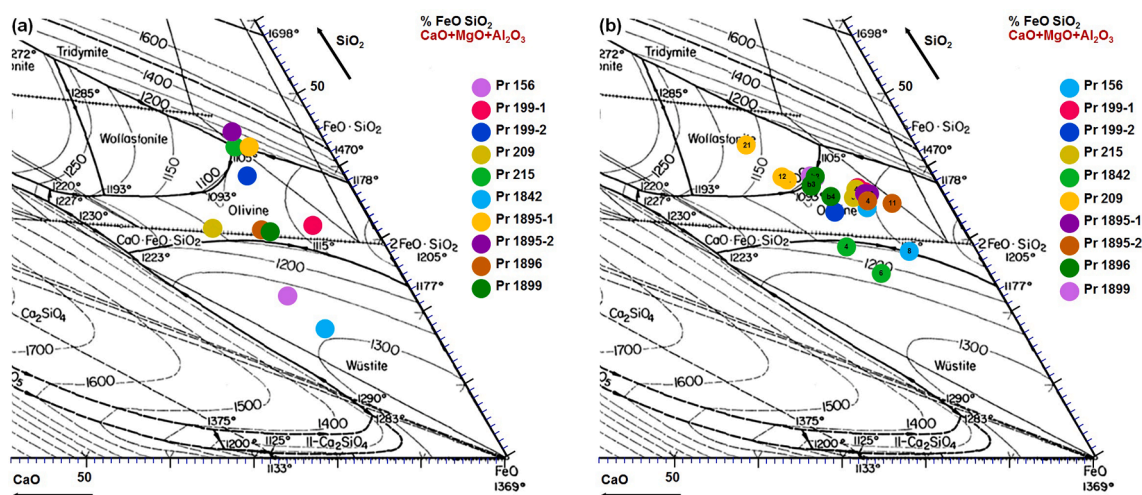
Fig. 3. Evaluation of the XRF analyses (a) and selected SEM-EDX area analyses. Representation of the analysed compositions in the FeO-SiO2-CaO phase diagram.

(Pr 156, Pr 1842).

The Cu content in the slags was between 0.3 and 1.2% by weight of CuO.

In four samples, Sn was detected, with a content of between 0.06 and 0.44 wt% SnO (Pr 199–2, Pr 215, Pr 1895–2, Pr 156).

On the metallographic sections, selected structures were characterised by means of SEMEDX surface analyses. These analysis results are also summarised in the FeO-SiO2-CaO phase diagram (Fig. 3b). The differences from the XRF measurements were due to the smaller analytical volumes of material analysed by SEM-EDX (Haubner, et al., 2017a). Most of the SEM-EDX measurement results showed lower SiO2 contents, since unmelted SiO2 grains were not recorded with this method.

The results of the metallographic examinations carried out are summarised and presented for each slag samples.

3.2. Plate slags of group 1 with compositions around the olivine-wollastonite-SiO2 ternary eutectic

Plate slag Pr 199–2 had a thickness of max. 0.48 cm with a

depression on one side. Analyses of selected cross-sections are compiled in Fig. 4. In LOM and SEM, very even structures could be seen, consisting of elongated fayalite aggregates (Fe2SiO4) surrounded by a glass phase (Fig. 4a-d). Within the glass phase there were local accumulations of copper-containing particles, which can be described as a transition state from ore to matte and metallic copper, and reaching sizes of up to 100 µm (Fig. 4d, f). In some regions of the slag, block-like olivine crystals were found (Fig. 4e). The dark areas in the interior of this olivine, observable in the SEM-BSE image, were due to increased Mg concentrations. The 0.06 wt% SnO detected by means of XRF could not be localised by means of SEM-EDX.

The structure of plate slag Pr 215, with a thickness of 0.22–0.25 cm, is shown in Fig. 5. The dendritic Fe2SiO4 crystals were arranged perpendicular to the surface and reached lengths of up to 1.8 mm (Fig. 5a, d). This could only be explained by the slag having melted completely and solidified relatively slowly without mechanical impact, allowing dendrite growth. At the top of the slag, where the melt solidified first, the structure was finer-grained and in the areas that solidified last, shrinkage holes had formed (Fig. 5d). In this sample too, bright copper containing patches were detected in the glass phase (Fig. 5b, c, e,
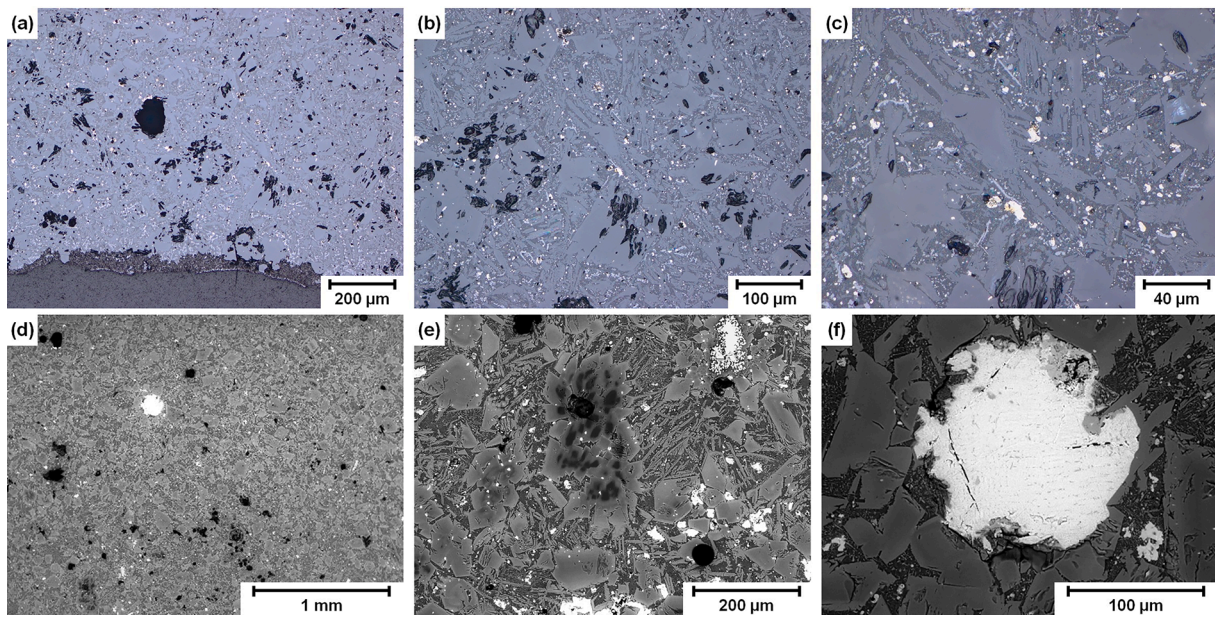
Fig. 4. Plate slag Pr-199-2: (a - c) cross section in LOM, (d - f) cross section in SEM.
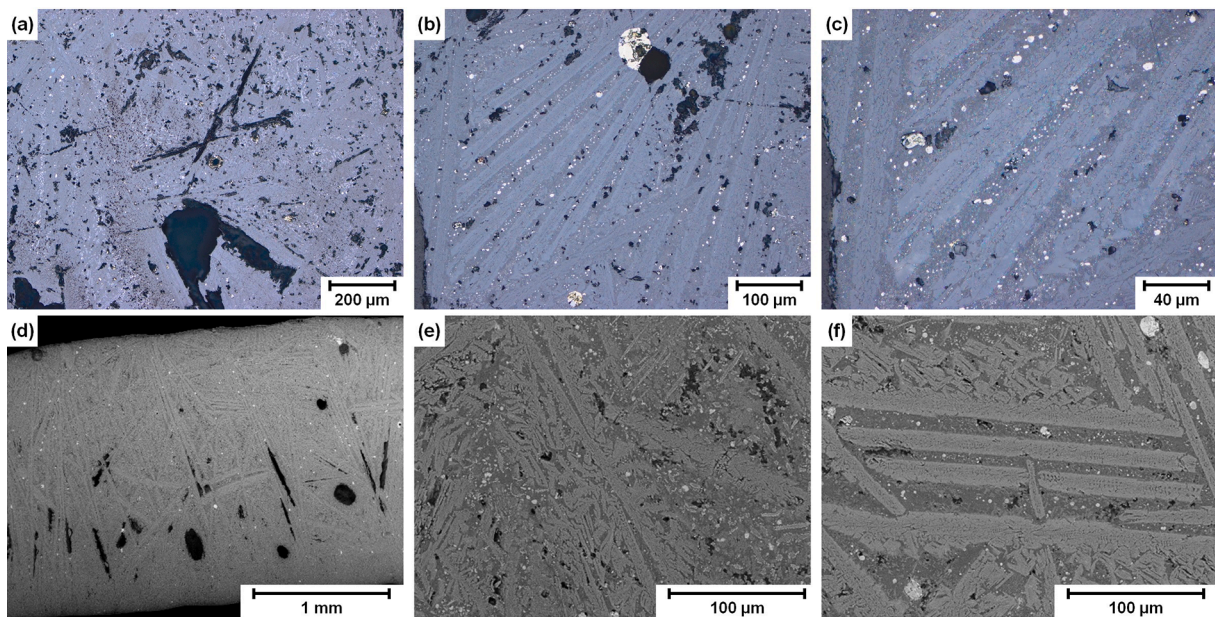

Fig. 5. Plate slag Pr-215: (a - c) cross section in LOM, (d - f) cross section in SEM.
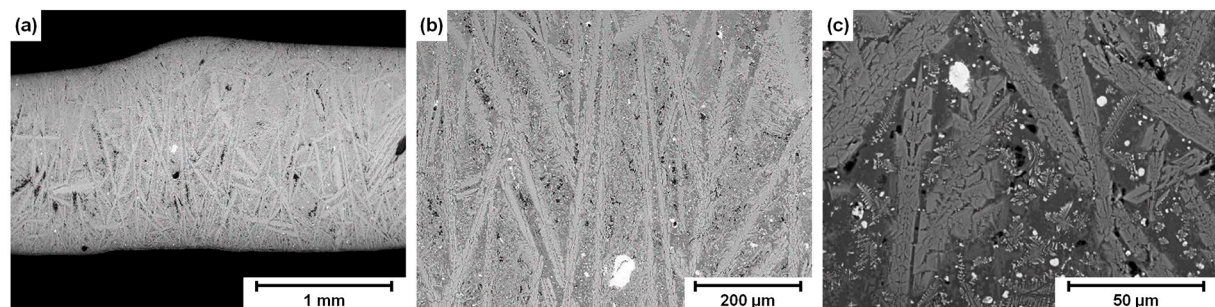

Fig. 6. Plate slag Pr 1895-1: (a - c) cross-section in SEM.

f).

Plate slag Pr 1895–1 was only 0.13–0.18 cm thick and had a uniform structure (Fig. 6). Long fayalite crystals were surrounded by a glass phase and, here too, copper containing particles and shrinkage holes from the solidification process could be observed.

Plate slag Pr 1895–2 had a thickness of 0.19–0.25 cm. The surface of this sample was examined as well as the metallographic sections (Fig. 7). Large hollows with a diameter of approx. 2 mm were detected (Fig. 7a) and long fayalite crystals could be seen, embedded in a glass phase (Fig. 7b). In some areas the fayalite crystals were well developed (Fig. 7c).

In the metallographic section, long fayalite crystals, a glass phase and shrink holes were observed (Fig. 7d). In some areas there were large or block-like olivine crystals from which fayalite crystals had begun to grow (Fig. 7e, f, i). Copper containing particles were also found in places (Fig. 7g, h).

3.3. Plate slags of group 2 with compositions at the olivine-wustite phase boundary

Slag Pr 199–1 was approx. 0.33–0.37 cm thick and had a uniform structure (Fig. 8a, b). In contrast to the structures described above, it contained block-like olivine crystals of up to 200 μm in size (Fig. 8c, d, e). Between these olivine crystals was a mixture of fayalite and glass phase, with fayalite bars reaching lengths of up to 200 μm. In the glass phase were particles with an increased Cu content (Fig. 8e, f).

Slag Pr 209 was a rim fragment (Fig. 9a) with a plate thickness of approx. 0.33 cm. Visible on the surface were both elongated crystals, corresponding to the fayalite plates in the structure (Fig. 9b) and square crystals, corresponding to the olivine (Fig. 9c). This surface structure

was presumably created by weathering of the amorphous glass phase. In the edge bulge (Fig. 9d, e) increased amounts of copper ore were observed, but otherwise the structure was very homogeneous. Blocky olivine crystals could occasionally be seen, surrounded by fayalite plates with lengths of up to 500 μm and a glass phase (Fig. 9f, h). Some shrinkage holes could be observed in areas of the glass phase (Fig. 9f, g).

Plate slag Pr 1896 had a beaded rim and a plate thickness of approx. 0.28 cm. The slag surface is rather smooth (Fig. 10a, b) and spalling can be seen in a few places (Fig. 10d). A special feature was a particle with a high Sn content, found on the surface of the slag (Fig. 10c, f). The surface of this Sn particle was largely covered with a layer of malachite (Fig. 10c, e). A SEM-EDX element distribution mapping (Fig. 10g) showed that Sn and O were present next to each other. Some S was found in the malachite as well. The structure was uniform (Fig. 11a, b) and, again, olivine crystals were found interspersed with fayalite plates and a glass phase (Fig. 11c, d). Occasionally, Cu-rich inclusions were detected, consisting of various phases (Fig. 11e). The bright veins seen in Fig. 11f are metallic Cu.

Slag Pr 1899 was a rim fragment with a thickness of 0.30 cm. The surface of this slag, too, featured square and elongated crystals (Fig. 12a, b, c). The structure was very uniform (Fig. 12d, e, g) but occasionally showed copper containing inclusions, up to 600 μm in size (Fig. 12g, h). Fayalite plates measuring up to 600 μm surrounded by a glass phase dominated the structure, but without block-like olivine crystals (Fig. 12f, i). Two SEM-EDX element distribution mappings were made, one of the slag structure, in order to show the distribution of the elements between the fayalite and the glass phase (Fig. 13a) and the other of a copper containing inclusion, to show the distribution of Cu, Fe, S and O (Fig. 13b).
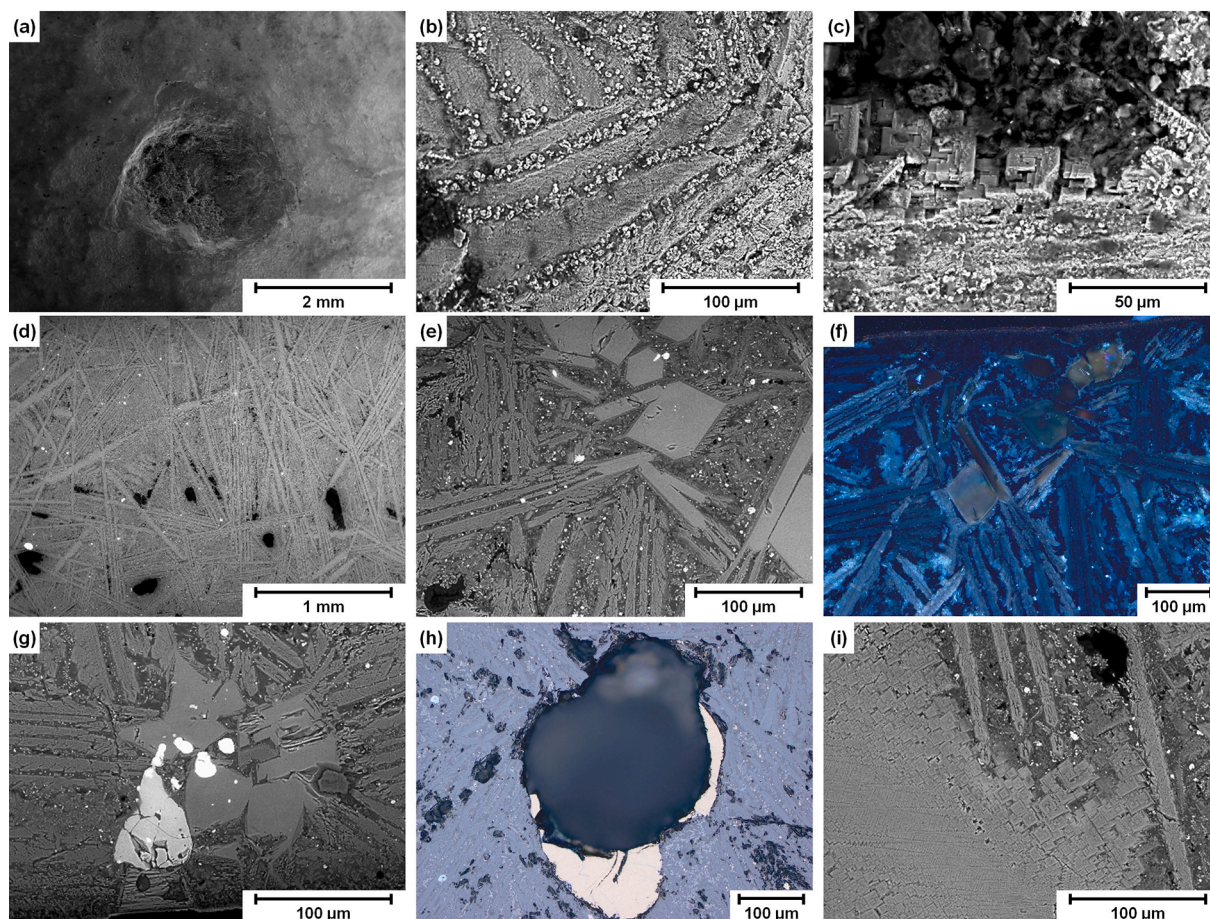

Fig. 7. Plate slag Pr 1895-2: (a – c) surface in SEM; (d, e, g, i) cross section in the SEM, (f, h) cross section in LOM.
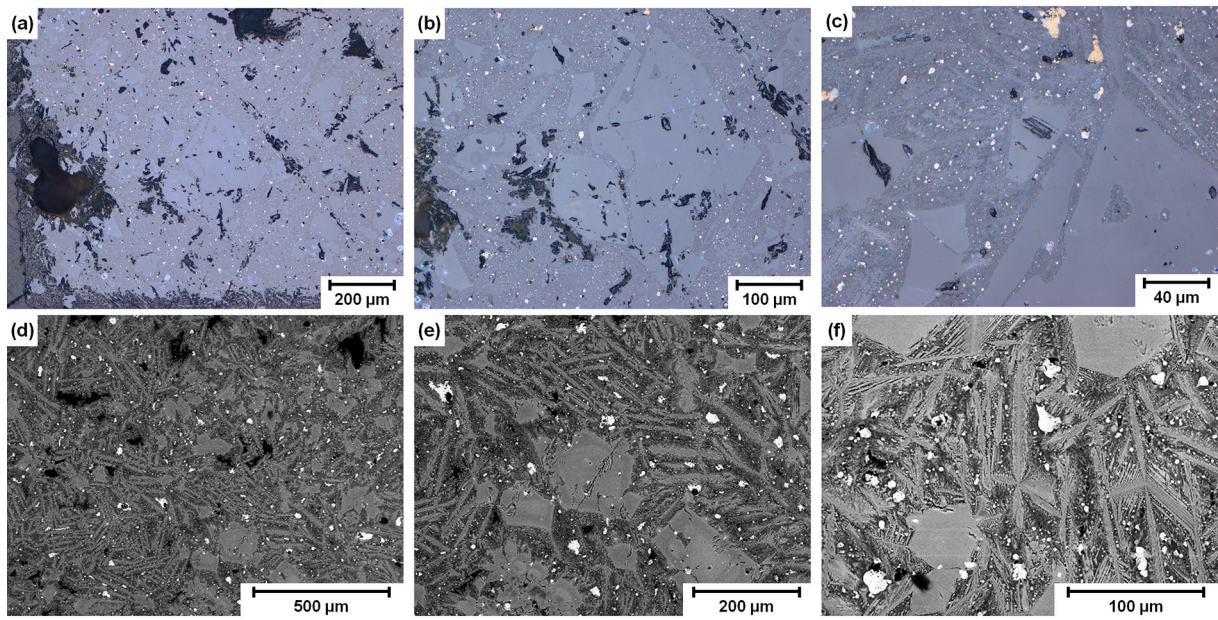
Fig. 8. Plate slag Pr 199-1: (a – c) cross section in LOM, (d - f) cross section in SEM.
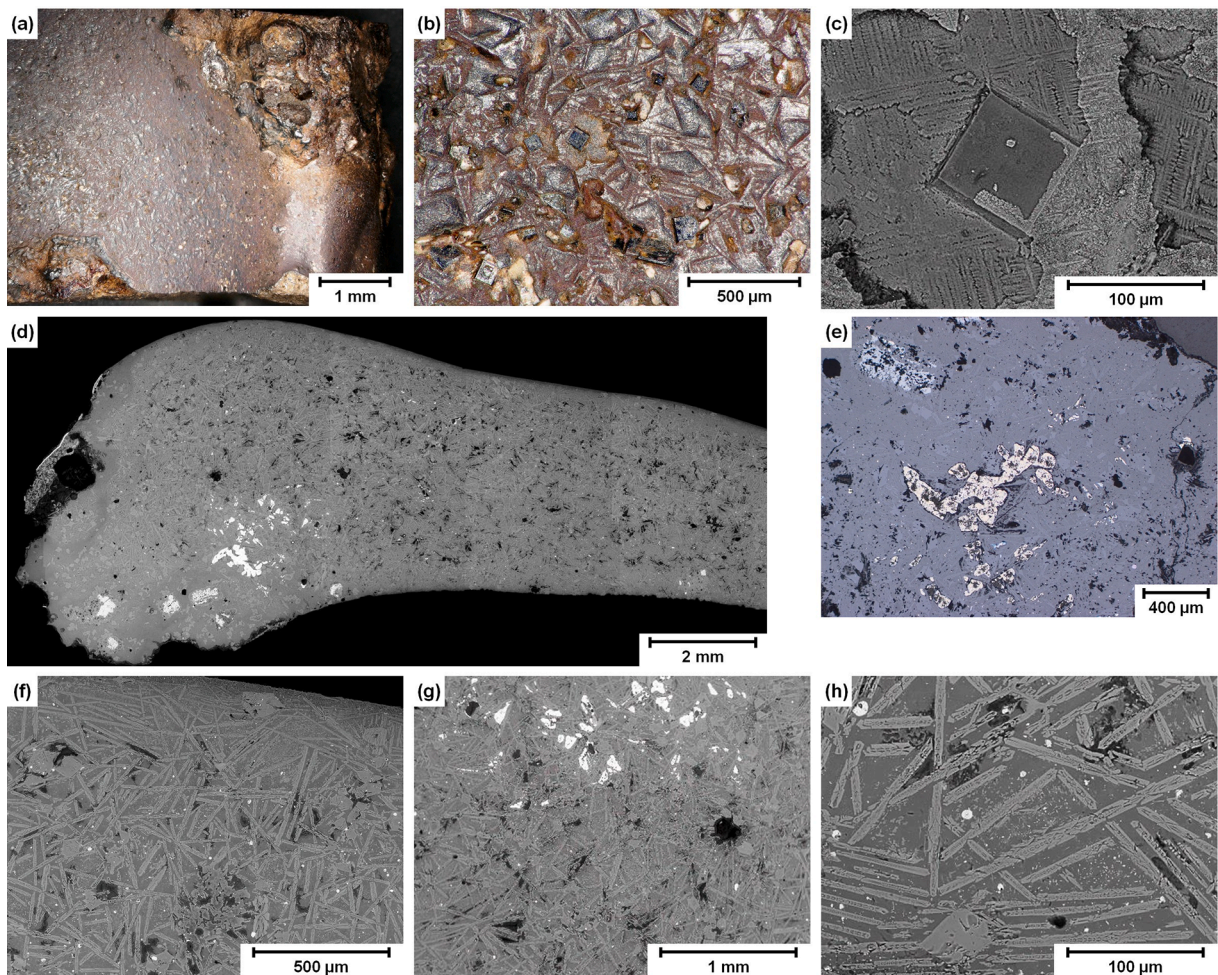

Fig. 9. Plate slag Pr 209: (a, b) surface in 3D-DM, (c) surface in SEM; (d) overview of an edge area in the SEM, (e) cross section in the LOM, (f - h) cross section in the SEM.
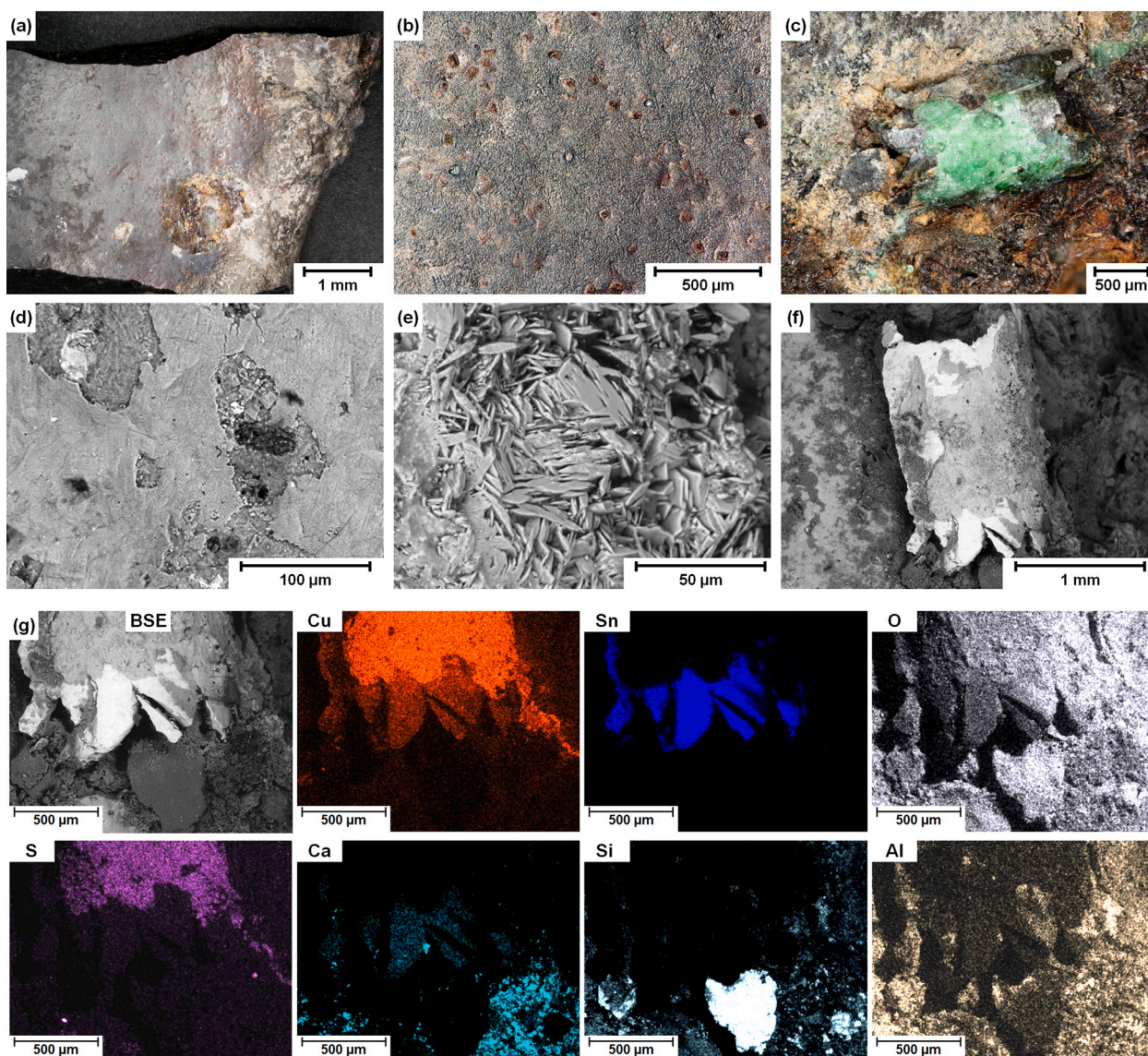
Fig. 10. Plate slag Pr 1896 with Sn-rich particle on the surface (c, f): (a - c) surface in 3D-DM, (d - f) surface in SEM; (g) SEM-EDX element distribution mapping of the particle with the high Sn concentration.

3.4. Plate slags of group 3 with compositions in the wüstite phase area

Slag Pr 156 had a thickness of 0.22–0.27 cm and a partially corrugated surface (Fig. 14a, b). In some areas, bright phases could be seen on the surface, consisting of block-like olivine crystals exposed by weathering (Fig. 14c). The structure of the slag was uniform, with only isolated cracks and small shrinkage holes (Fig. 14d, e). The visible fayalite crystals in the structure were relatively short compared to the other slags, measuring up to 100 µm (Fig. 14f). According to the XRF measurements, the Fe concentration in this slag was high and this iron can be present in increased amounts in the fayalite or finely distributed in the glass phase.

Pr 1842 had a plate thickness of 1.03 cm. Again, the slag was characterized by a uniform structure and misshapen shrinkage holes (Fig. 15a). The rather rounded pores could also be explained by the evolution of gas during the solidification of the melt. The length of the fayalite crystals was approx. 100 µm, although there was a relatively large amount of glass phase (Fig. 15b). FeO dendrites or pellets could be found in the glass phase (Fig. 15c - e) and spherical Cu-enriched inclusions were also observed (Fig. 15e, f).

4. Discussion

4.1. Slag structure and metallurgical process

The structure of the slags was determined by their chemical composition and their cooling rate during solidification. Phases and processes during solidification could be roughly estimated from a simplified representation of slag composition in the $FeO-SiO_2-CaO$ phase diagram (Haubner, et al., 2017a). However, the melting-temperature range of the slag and the influence on this of other elements had to be taken into account. The dendritic morphology of the fayalite was also determined by the cooling rate of the slag during solidification (Ettler, et al., 2009).

From the point of view of the metallurgical process itself, a low melting point of the slag was desirable, in order to achieve a low slag viscosity and a good separation between the molten metal and the slag, especially given the melting points of copper (1085 °C) and bronze (950–800 °C) with about 10% by weight Sn (MASSALSKI, 1990). However, it can be assumed that the slags on the surface of the molten metal had already solidified before they were lifted off.

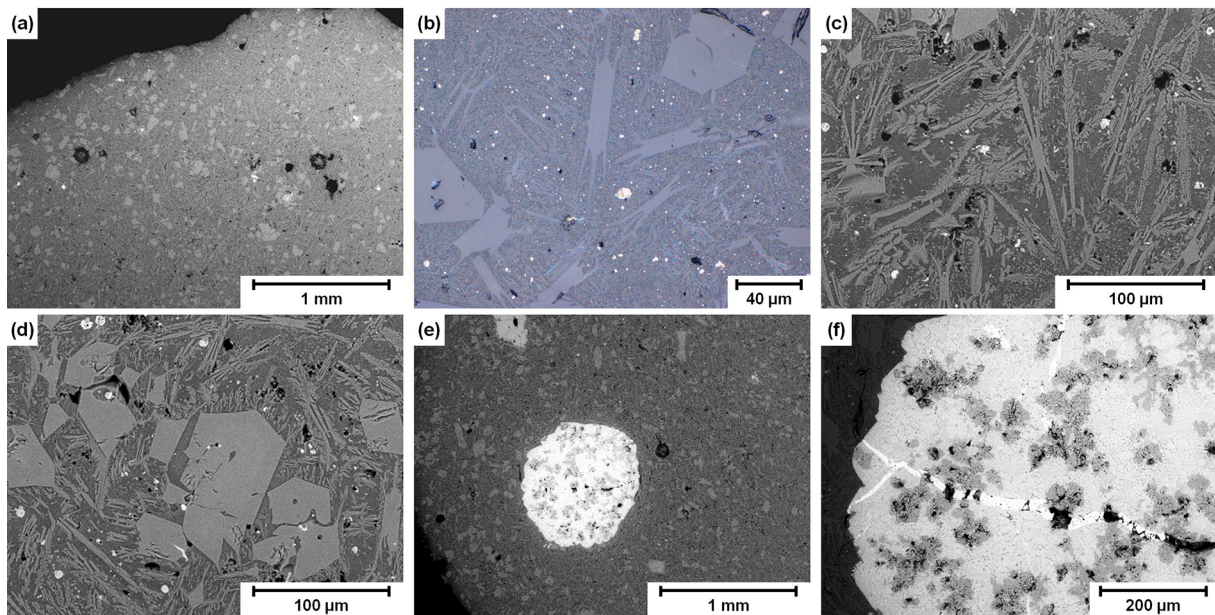The exact composition of the olivine is unknown, because both Ca

Fig. 11. Plate slag Pr 1896: (a, c – f) cross section in SEM, (b) cross section in LOM.
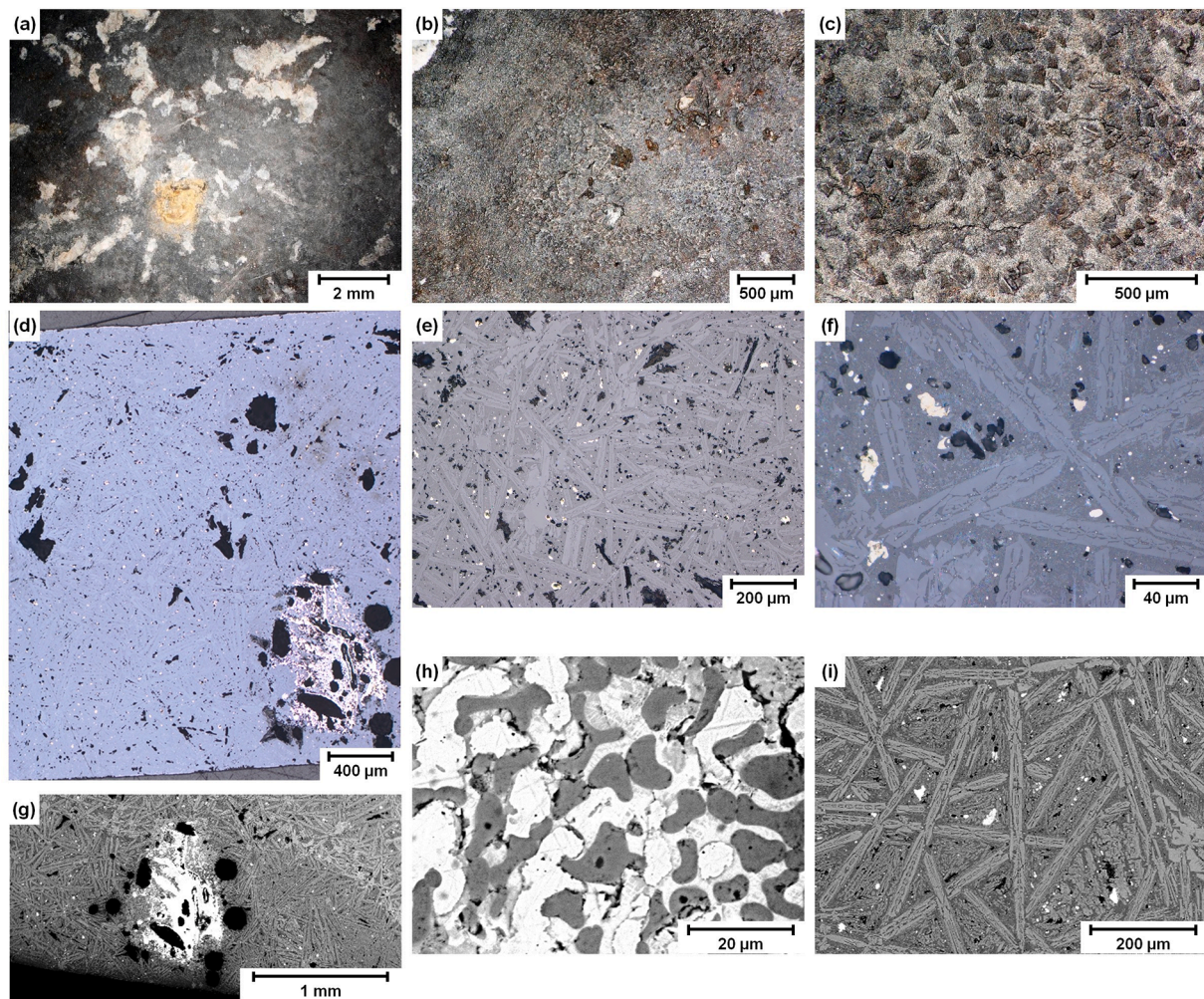

Fig. 12. Plate slag Pr 1899: (a - c) surface in the 3D-DM; (d, f) cross section in LOM; (e, g - i) cross section in SEM.
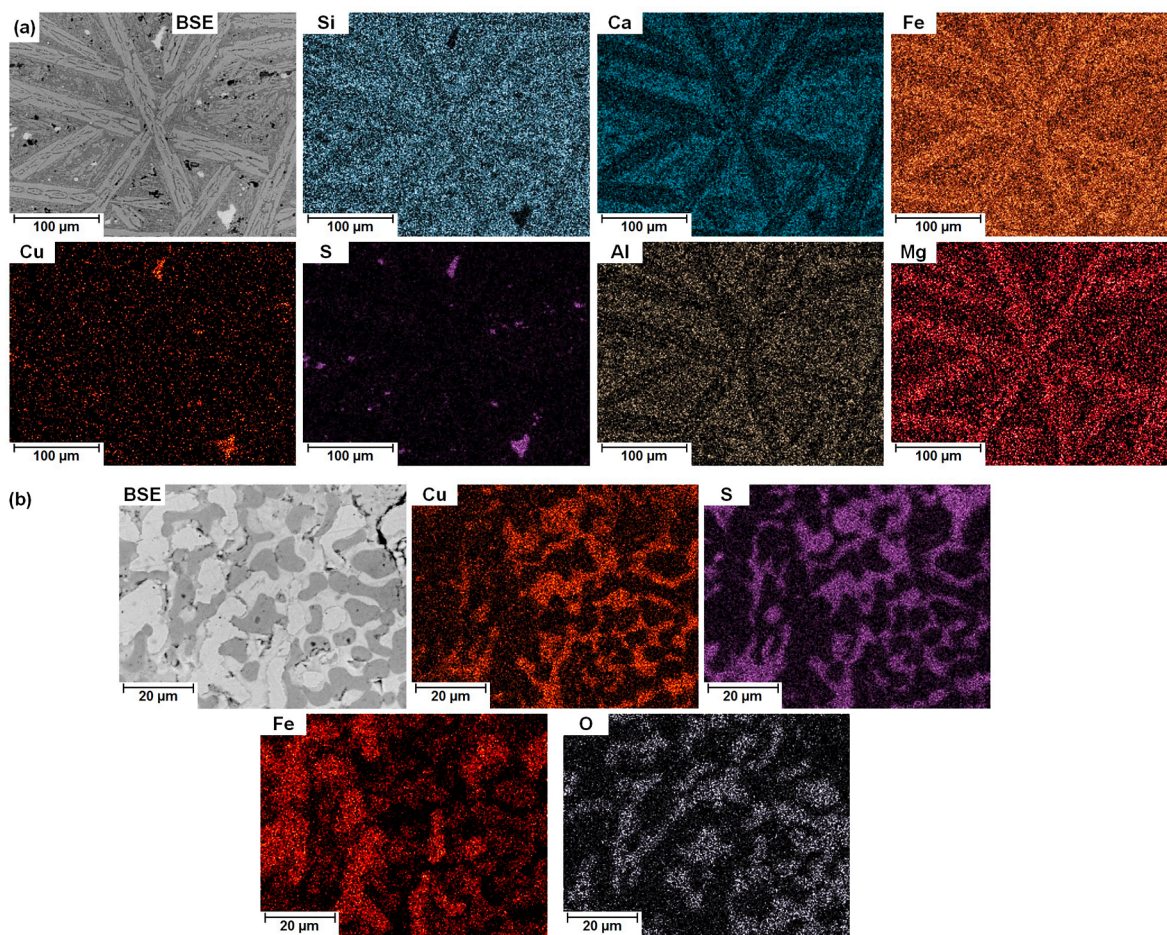
Fig. 13. Plate slag Pr 1899: SEM-EDX element distribution mappings (a) homogeneous slag area; (b) Cu-rich inclusion.
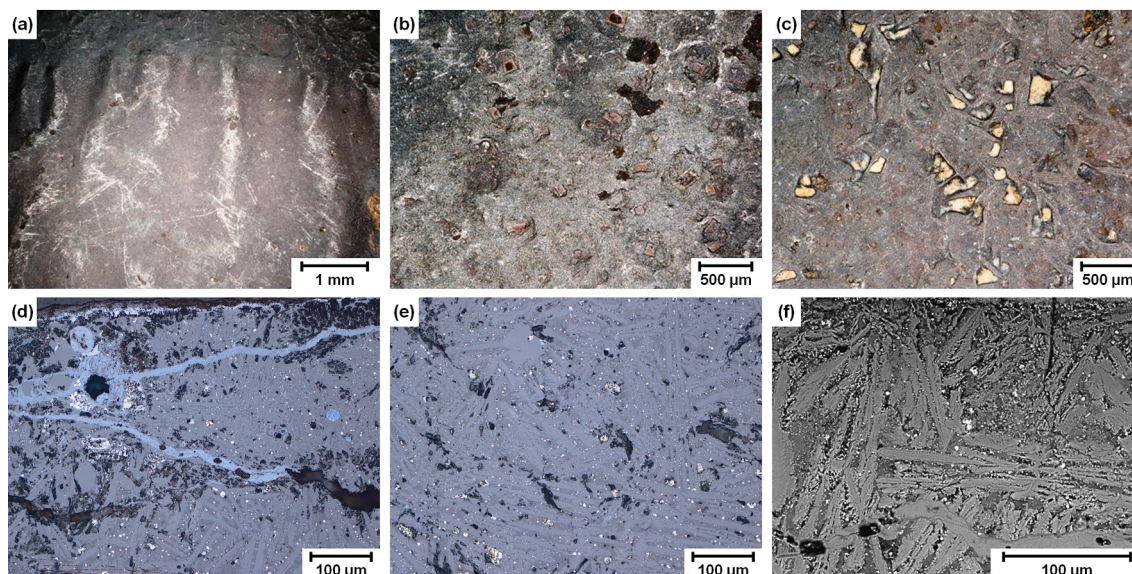

Fig. 14. Plate slag Pr 156: (a – c) surface in 3D-DM, (d, e) cross section in LOM, (f) cross section in SEM.

and Fe can be substituted by other elements, meaning that many variants are possible. Fayalite (Fe_2SiO_4) is a type of olivine that contains only Fe. Other types are, e.g., forsterite Mg_2SiO_4, tephroite Mn_2SiO_4, kniebelite $(Fe, Mn)_2SiO_4$, kirschsteinite $CaFeSiO_4$, and monticellite $CaMgSiO_4$ (Devic and Marceta, 2007).

The composition of the slags designated as group 1 was close to the ternary eutectic olivine-wollastonite- SiO_2 (1105° C) in the FeO-SiO_2-CaO phase diagram (Pr 199–2, Pr 215, Pr 1895–1, Pr 1895–2). Since there were no SiO_2 aggregates in the structure, the solidification process could be reconstructed as follows. It started with the separation of
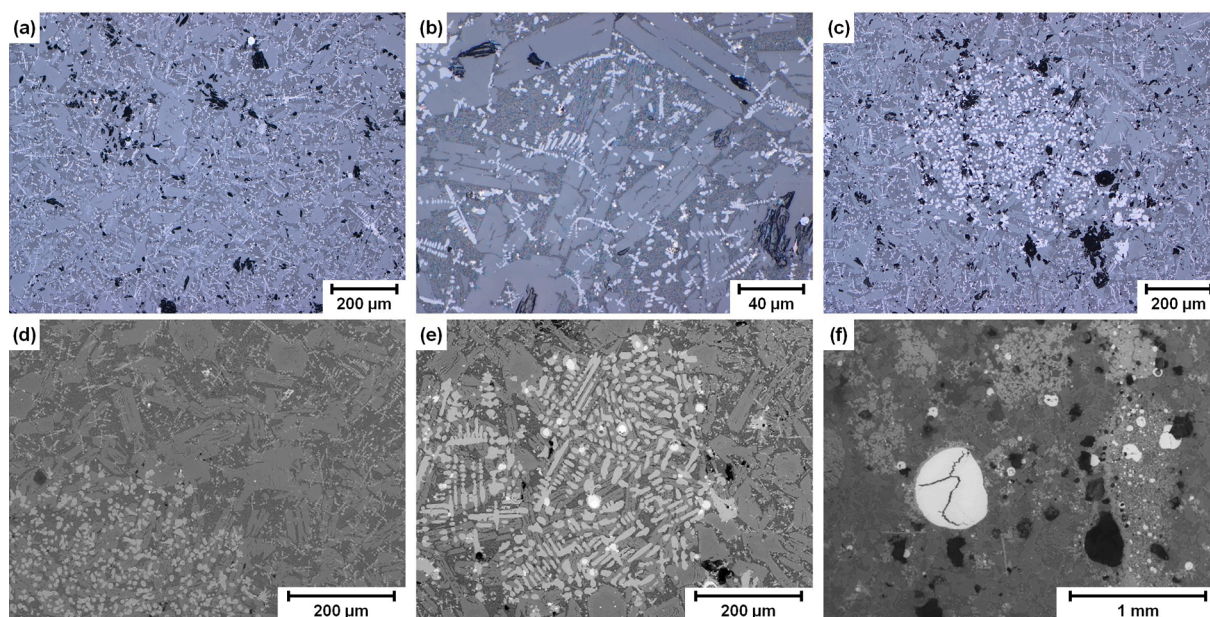
Fig. 15. Plate slag Pr 1842: (a – c) cross section in LOM, (d - f) cross section in SEM.

olivine, with Mg preferably incorporated, in addition to Fe, in the initial phase. Subsequently, Fe-enriched olivine (fayalite) was precipitated. At the ternary eutectic, fayalite and the glass phase were formed. The closer the composition of the melt was to the ternary eutectic, the longer the fayalite crystals became. There were also residues of various copper phases in the glass phase. Due to the decrease in volume during the solidification of the melt, shrinkage holes appeared in the area of the glass phase, because it solidified last.

Group 2: Composition at the olivine-wustite phase boundary (1100–1150° C) (Pr 199–1, Pr 209, Pr 1896, Pr 1899). Since very long fayalite crystals were observed in these slags, extending across almost the entire thickness of the slag, it can be assumed that a very homogeneous slag melt solidified from the top downwards. The other impurities in the melt formed the glass phase, in which residues of small copper containing particles were also included. In some cases, block-like olivine crystals were found, which served as seeds for the fayalite crystals (Fig. 7e, f).

The slags of group 3 contained higher concentrations of FeO and their composition was therefore in the phase range of wustite (1250–1300° C) (Pr 156, Pr 1842) (Klemm et al., 2013; Haubner and Strobl, 2014). In these samples, FeO was present in the form of local accumulations (Fig. 15c, d), in which the FeO could be spherical (Fig. 15c, e, d) or dendritic (Fig. 15e). Aside from these enrichments, it could be seen that FeO solidified first, in dendritic form, followed by fayalite and finally by the glass phase (Fig. 15b). Some of the FeO dendrites had developed into fayalite, meaning that the fayalite crystals continued to grow during the solidification of the residual melt while the glass phase was also being precipitated.

4.2. Cu-containing particles

Cu-containing particles of different sizes were also found. SEM-EDX measurements showed that these were particles in various stages of the reduction process (Fig. 4f, Fig. 7g, Fig. 9e, Fig. 11e, Fig. 12d, g, h). Some, corresponding to the bright veins in the SEM, were already reduced to metallic Cu (Fig. 11f). A SEM-EDX element distribution mapping of Cucontaining particles (Fig. 12g, h) showed that Cu was preferably associated with S and Fe was preferably associated with O (Fig. 13b). A precise phase analysis was not possible due to the small size of the particles, but the composition was probably a mixture of chalcopyrite, digenite (Cu_9S_5), bornite (Cu_5FeS_4) and wustite (FeO) (Shishin, et al.,

2015). These inclusions confirmed that local ores – mainly chalcopyrite and pyrite – were processed at the Prigglitz-Gasteil site (for the local ore mineralization see HACKENBERG, 2003; Niedermayr, et al., 2014; pers. comm. Michael Götzinger, Institute for Mineralogy and Petrography, University of Vienna; analyses of a series of copper ores from Bronze Age contexts at the Prigglitz-Gasteil site by Peter Tropper and Lena Oettel are under way at the University of Innsbruck's Institute of Mineralogy).

Due to the lower density of the slag compared to molten metal, the copper containing particles were found in the slag. The average Cu content of the bulk samples (0.59 wt%) was mainly due to the copper containing particles, because no metallic Cu droplets were observed in any of the samples. This shows that during the smelting process, Cu was very well separated from the slag.

The average Cu content of the Prigglitz samples was a little lower than at other Late Bronze Age copper smelting sites. An average of 0.95 wt% Cu was measured from 18 plate slags from the Palten and Johnsbach Valleys in Upper Styria (Presslinger and Eibner, 2014). The slag cakes and plate slags from Trentino in northern Italy contained 1 wt% Cu on average, in the form of 1–2 mm diameter copper matte (METTEN, 2003). Metallic copper inclusions were also detected in slag cakes and plate slags from the Late Bronze Age smelting site of Mauk A in the Tyrol, with plate slags containing up to ca. 1 wt% Cu and the slag cakes containing as much as some percent of Cu (Krismer, et al., 2015). Late Bronze Age smelters in these regions crushed the slags in order to recover the copper prills, thus producing a large amount of "slag sand" (REITMAIER-NAEF, 2019).

4.3. Tin in the bulk and on the surface of plate slags

Between 0.06 and 0.44 wt% SnO was measured in four slags by means of XRF (Pr 199–2, Pr 215, Pr 1895–2, Pr 156). In the SEM-EDX investigations, however, no Sn accumulations were found; either the Sn had an extremely fine distribution within the structure or by chance there were no accumulations in the samples analysed.

A survey of published chemical bulk analyses of plate slags from the Alpine region showed that no Sn was found in plate slags in the Trentino region (Italy), at Mühlbach am Hochkönig in Salzburg (Austria), in the Palten and Johnsbach Valleys in Styria (Austria) or in the Mauken district in the Lower Inn Valley in Tyrol (Austria), (METTEN, 2003; Presslinger and Eibner, 2014; Krismer, et al., 2015).

The presence of Sn in some plate slags from Prigglitz-Gasteil can on

the one hand be explained by the occurrence of small concentrations of Sn in the local ore, but on the other hand the Sn could also have entered the slag during the alloying of copper with tin (Montes-Landa, et al, 2020; Rademakers and Farci, 2018). Montes-Landa et al. 2020 summarized the five ways bronze can be made, which could also result in Sn getting into the slag:

1. Natural alloying using polymetallic Cu-Sn ore.
2. Co-smelting of copper minerals with cassiterite.
3. Alloy formation under reducing conditions of metallic copper with cassiterite.
4. Co-melting of metallic copper with metallic tin.
5. Re-melting respectively recycling of bronze scrap.

Among the investigated copper ore samples (mainly chalcopyrite and pyrite) from Prigglitz-Gasteil, cassiterite has been detected in very small amounts (Niedermayr, et al., 2014). Sn was also detected as a minor trace element with 244 ppm on average (Mödlinger, et al., 2021). It can probably be ruled out that the Sn content in the slag is due to the low Sn content in the ore, because then all slag would have to contain Sn. Another possibility for the traces of tin to get into the thin plate slag would have been during the process of refining matte while adding scrap bronze metal that was abundantly available at the workplace.

Surprisingly, a particle with a high Sn content was detected on the surface of plate slag Pr 1896 (Fig. 10c, f). An SEM-EDX element distribution mapping (Fig. 10g) showed that it was probably SnO_2. The question was whether Sn bronzes were obtained by alloying Cu with metallic Sn or by adding SnO_2 to the Cu melt (Rademakers and Farci, 2018). A clear answer based on our measurements was not possible, because any metallic Sn which was used for alloying could have been oxidized to SnO_2 by weathering. The surface of this Sn-enriched particle was extensively covered with a malachite layer (Fig. 10d, e), also containing some S, presumably SO_4^{2-}. In fact, the plate-slag samples from Prigglitz-Gasteil were found in the context of bronze casting residues such as casting drops, a casting sprue and fragmented casting moulds for bronze objects (Haubner et al., 2017; Haubner et al., 2019; Mödlinger, et al., 2021; Mödlinger and Trebsche, 2021). Hence, the presence of a tin particle on the surface of a plate slag that was otherwise tin-free (as measured by XRF) most probably is the result of a contamination with material from a nearby foundry workshop.

4.4. The surfaces of the plate slags

The surfaces of some slags were also examined. In general, these surfaces were strongly influenced by weathering. The structure of the slags was in part already visible, because the amorphous or fine-grained glass phase was more weathered than the crystals.

Particularly noticeable were bright (Fig. 14c) or square crystals (Fig. 9b, c) that had been exposed to weathering (Fig. 10b). These were coarse olivine crystals, which had been the first to crystallize out during solidification and were therefore closer to the surface. In addition, there were elongated fayalite crystals (Fig. 7b, Fig. 9b). Even finer particles could be seen in the corroded areas of the glass phase, but their composition was not determined (Fig. 7b, c).

The slag surfaces were often rough (Fig. 9a, Fig. 10a) and inhomogeneous, especially in the area of the edge bulge.

5. Conclusions

The investigated plate slag fragments from the mining settlement Prigglitz-Gasteil were rather thin (0.13–1.03 cm, mean 0.32 cm) and macroscopically homogeneous, showing that the slags had been completely melted and had formed during the processing of copper ores. They contained small copper containing particles, indicating that local copper ores were processed at the site.

The slags could be divided into three groups, according to their chemical compositions. The slags of group 1 contained more SiO_2 than the others and their chemical composition was located around the

ternary eutectic olivine-wollastonite- SiO_2 in the FeO-SiO_2-CaO phase diagram. The compositions of group 2 were located at the olivine-wustite phase boundary, and more Fe was measured in group 3, which meant that the composition lay in the wustite phase region.

The structures of the slags differed in their phase compositions, i.e., in the ratios of olivine, fayalite, glass phase, and, in the case of group 3 slags, wustite. They must therefore have solidified at slightly different temperatures (from ca. 1100 to ca. 1300° C). However, these differences were not the result of separate stages during the working process but simply of haphazard variations. This was confirmed by the fact that no significant differences were observed in terms of slag composition, thickness, Cu or Sn content between the two investigated terrain terraces (T3 and T4), located at a distance of ca. 60 m from each other.

Moreover, only very small amounts of copper containing residues were observed in all the plate slags (average Cu content 0.59 wt%), indicating an efficient process of copper smelting, comparable with other copper production sites in the Eastern Alps. Remarkably, four out of ten plate slags also contained tin (0.06–0.44 wt%) which could result from mixing bronze scrap metal with matte during the process of refining. Furthermore, a tin particle on the surface of another plate slag obviously represents a workshop contamination with the nearby bronze foundry, proving that primary and secondary metallurgy were carried out in immediate vicinity.

The surfaces of the slags were corroded, resulting in the removal of the glass phase and leaving block-like olivine and elongated fayalite crystals clearly visible.

It should be pointed out that the slags examined here originate from the last copper smelting step, or the bronze production step. The previous production steps of copper extraction were proven in Prigglitz-Gasteil, but were not the subject of these investigations.

Declaration of Competing Interest

The authors declare that they have no known competing financial interests or personal relationships that could have appeared to influence the work reported in this paper.

Data availability

No data was used for the research described in the article.

References

Devic, S., Marceta, L., 2007. Differences in morphological properties between the olivine group minerals formed in natural and industrial processes. J. Min. Metall. 43B, 99–105.

Ettler, V., Červinka, R., Johan, Z., 2009. Mineralogy of medieval slags from lead and silver smelting (Bohutín, Příbram district, Czech Republic): Towards estimation of historical smelting conditions. Archaeometry 51 (6), 987–1007.

Hackenberg, M., 2003. Bergbau im Semmeringgebiet. Archiv für Lagerstättenforschung der Geologischen Bundesanstalt, Vienna, pp. 5–97.

Hampl, F., Mayrhofer, R.J., 1958. Die ur- und frühgeschichtliche Bergbauforschung in Niederösterreich. In: Studia Palaeometallurgica in Honorem Ernesti Preuschen (Archiv für ur- und frühgeschichtliche Bergbauforschung Nr. 12). Archaeologia Austriaca, Beiheft 3, 46–56.

Hanning, E., Herdits, H., Silvestri, E., 2015. Alpines Kupferschmelzen – technologische Aspekte. In: T. Stöllner, K. Oeggl, eds. Bergauf Bergab. 10.000 Jahre Bergbau in den

Ostalpen. Wissenschaftlicher Beiband zur Ausstellung im Deutschen Bergbau-Museum Bochum vom 31.10.2015-24.04.2016. Im vorarlberg museum Bregenz vom 11.06.2016-26.10.2016. Bochum: Verlag Marie Leidorf, pp. 225–231.

Haubner, R., Strobl, S., 2014. Slag investigation from iron smelting and iron processing sites in Austria – from Hallstatt and medieval period and the 19th century. Mater. Sci. Forum 782, 635–640.

Haubner, R., Strobl, S., Klemm, S., Trebsche, P., 2015. Prähistorische Kupfergewinnung im südöstlichen Niederösterreich – archäometallurgische Untersuchungen an alten und neuen Fundstücken. In: E. LAUERMANN, P. TREBSCHE, eds. Beiträge zum Tag der Niederösterreichischen Landesarchäologie 2015. Asparn/Zaya: Niederösterreichisches Landesmuseum, pp. 26–33.

Haubner, R., Strobl, S., Klemm, S., 2017a. Investigations of a slag from copper smelting discovered at the Bronze Age site Prein VII/Cu in Lower Austria. In: I. MONTERO-RUIZ, A. PEREA, eds. Archaeometallurgy in Europe IV. Bibliotheca Praehistorica Hispana, 33. Madrid: Editorial CSIC, pp. 135–142.

Haubner, R., Strobl, S., Trebsche, P., 2019. Metallographic analyses from the late Urnfield period copper mining settlement at Prigglitz-Gasteil in Lower Austria. In: Turck, R., Stöllner, T., Goldenberg, G., eds. Alpine Copper II – Alpenkupfer II – Rame delle Alpi II – Cuivre des Alpes II. New Results and Perspectives on Prehistoric Copper Production. Bochum: Verlag Marie Leidorf, pp. 323–332.

Haubner, R., 2021. Die prähistorische Kupfermetallurgie – allgemeine Betrachtungen. BHM Berg- und Hüttenmännische Monatshefte, 166(7), 343–351.

Hauptmann, A., 2014. The Investigation of Archaeometallurgical Slag. In: B.W. ROBERTS, C.P. THORNTON, eds. Archaeometallurgy in Global Perspective. Methods and Syntheses. New York, Heidelberg, Dordrecht, London: Springer Science+ Business Media, pp. 91–105.

Hodoroaba, V.-D., 2020. Energy-dispersive X-ray spectroscopy (EDS). In: Characterization of Nanoparticles. Elsevier, pp. 397–417.

Haubner, R., Strobl, S., Trebsche, P., 2017. Analysis of Urnfield period bronze droplets formed during casting. Mater. Sci. Forum 891, 41–48.

Heiss, A.G., Jakobitsch, T., Wiesinger, S., Trebsche, P., 2021. Dig out, dig in! plant-based diet at the late bronze age copper production site of Prigglitz-Gasteil (Lower Austria) and the relevance of processed foodstuffs for the supply of Alpine Bronze Age miners. PLoS One 16, e0248287.

Herdits, H., 2017. Die ostalpine bronzezeitliche Kupfererzeugung im überregionalen Vergleich am Grundbeispiel eines Hüttenplatzes in Mühlbach/Sbg. Doctoral Thesis, University of Vienna.

Klemm, S., Strobl, S., Haubner, R., 2013. Mediaeval Iron Smelting in the Area of the Iron Mountain (Steirischer Erzberg) at Eisenerz, Styria (Austria). In: Mining in European History and its Impact on Environment and Human Societies. Innsbruck: Innsbruck University Press, pp. 103–109.

Kraus, S., Schröder, C., Klemm, S., Pernicka, E., 2015. Archaeometallurgical studies on the slags of the Middle Bronze Age copper smelting site S1, Styria, Austria. In: Hauptmann, A., Modarressi-Tehrani, D., eds. Archaeometallurgy in Europe III. Proceedings of the 3rd International Conference, Deutsches Bergbau-Museum Bochum, June 29 – July 1, 2011. Bochum: Deutsches Bergbau-Museum, pp. 301–308.

Krismer, M., Goldenberg, G., Tropper, P., 2015. Mineralogical-petrological investigations of metallurgical slags from the Late Bronze Age fahlore-smelting site Mauken (Tyrol, Austria). In: Hauptmann, A., Modarressi-Tehrani, D., eds. Archaeometallurgy in Europe III. Proceedings of the 3rd International Conference, Deutsches Bergbau-Museum Bochum, June 29 – July 1, 2011. Bochum: Deutsches Bergbau-Museum, pp. 309–318.

Lang, R., 2000. KG Prigglitz. Fundberichte aus Österreich, 39, 596–598.

Larreina-Garcia, D., Cech, B., Rehren, T., 2015. Copper smelting in the Raxgebiet (Austria): A Late Bronze Age Alpine Industrial Landscape. In: Suchowska-Ducke, P., Scott Reiter, S., Vandkilde, H., eds. Forging Identities. The Mobility of Culture in Bronze Age Europe. Volume 1. Oxford: British Archaeological Reports Ltd, pp. 213–219.

Massalski, T.B., 1990. Binary Alloy Phase Diagrams. ASM International, Metals Park OH.

Metten, B., 2003. Beitrag zur spätbronzezeitlichen Kupfermetallurgie im Trentino (Südalpen) im Vergleich mit anderen prähistorischen Kupferschlacken aus dem Alpenraum. Bochum: Deutsches Bergbau-Museum.

Mödlinger, M., Trebsche, P., 2021. Work on the cutting edge: metallographic investigation of Late Bronze Age tools in southeastern Lower Austria. Archaeol. Anthropol. Sci. 13, 125. https://doi.org/10.1007/s12520-021-01378-1.

Mödlinger, M., Trebsche, P., Sabatini, B., 2021. Melting, smelting, and recycling: A regional study around the Late Bronze Age mining site of Prigglitz-Gasteil, Lower Austria. PLoS ONE 16, e0254096.

Montes-Landa, J., Montero-Ruiz, I., Castanyer Masoliver, P., SANTOS Retolaza, M., Tremoleda Trilla, J., Martinón-Torres M., 2020. Traditions and innovations: versatility of copper and tin bronze making recipes in Iron Age Emporion (L'Escala, Spain). Archaeological and Anthropological Sciences 12:124.

Niedermayr, G., Auer, C., Berger, A., Bernhard, F., Bojar, H.-P., Brandstätter, F., Fink, R., Hollerer, C.E., Kolitsch, U., Mörtl, J., Postl, W., Prasnik, H., Schabereiter, H., Schillhammer, H., Steinwender, C., Strobl, M., Taucher, J., Walter, F., 2014. Neue Mineralfunde aus Österreich LXIII. Carinthia II 204./124, 65–146.

Pernicka, E., Lutz, J., Stöllner, T., 2016. Bronze Age Copper Produced at Mitterberg, Austria, and its Distribution. Archaeologia Austriaca 100, 19–55.

Piel, M., Hauptmann, A., Schröder, B., 1992. Naturwissenschaftliche Untersuchungen an bronzezeitlichen Kupferverhüttungsschlacken von Acqua Fredda/Trentino. In: A. LIPPERT, K. SPINDLER, eds. Festschrift zum 50jährigen Bestehen des Institutes für Ur- und Frühgeschichte der Leopold-Franzens-Universität Innsbruck. Bonn: Dr. Rudolf Habelt GmbH, pp. 463–472.

Presslinger, H., Eibner, C., 2013/2014.. Metallographische und mikroanalytische Beurteilungsergebnisse von bronzezeitlichen Erz-, Schlacken- und Rohproduktproben. Schild von Steier 26, 316–323.

Presslinger, H., Eibner, C., 2014. Der Beginn der Metallzeiten im Bezirk Liezen – eine montanarchäologische Dokumentation. Trautenfels.

Presslinger, H., Prochaska, W., 2002. Chemische Analysen von bronzezeitlichen Laufschlacken. Res Montanarum 28, 10–14.

Rademakers, F.W., Farci, C., 2018. Reconstructing bronze production technology from ancient crucible slag: experimental perspectives on tin oxide identification. J. Archaeol. Sci. Rep. 18, 343–355.

Reitmaier-Naef, L., 2019. Copper smelting slag from the Oberhalbstein (Canton of Grisons, Switzerland). Methodological considerations on typology and morphology. In: R. TURCK, T. STÖLLNER, G. GOLDENBERG, eds. Alpine Copper II – Alpenkupfer II – Rame delle Alpi II – Cuivre des Alpes II. New Results and Perspectives on Prehistoric Copper Production. Bochum: Verlag Marie Leidorf, pp. 229–244.

Shishin, D., Jak, E., Decterov, S.A., 2015. Thermodynamic assessment and database for the Cu–Fe–O–S system. CALPHAD: Comput. Coupling Phase Diagrams Thermochem. 50, 144–160.

Stöllner, T., 2015. Der Mitterberg als Großproduzent für Kupfer in der Bronzezeit. In: T. Stöllner, K. Oeggl, eds. Bergauf Bergab. 10.000 Jahre Bergbau in den Ostalpen. Wissenschaftlicher Beiband zur Ausstellung im Deutschen Bergbau-Museum Bochum vom 31.10.2015-24.04.2016. Im vorarlberg museum Bregenz vom 11.06.2016-26.10.2016. Bochum: Verlag Marie Leidorf, pp. 175–186.

Trebsche, P., Pucher, E., 2013. Urnenfelderzeitliche Kupfergewinnung am Rande der Ostalpen. Erste Ergebnisse zu Ernährung und Wirtschaftsweise in der Bergbausiedlung von Prigglitz-Gasteil (Niederösterreich). Prähistorische Zeitschrift 88, 114–151. https://doi.org/10.1515/Pz-2013-0004.

Trebsche, P., Weixelberger, G., 2022. A mining subsidence event around 920 BC in the Late Bronze Age copper mine of Prigglitz-Gasteil (Lower Austria). Archäologisches Korrespondenzblatt 52/1.

Trebsche, P., Schlögel, I., Flores-Orozco, A. 2022. Combining geophysical prospection and core drilling: reconstruction of a Late Bronze Age copper mine at Prigglitz-Gasteil in the Eastern Alps (Austria). Archaeological Prospection, submitted.